Science of the Total Environment 811 (2022) 151408

Contents lists available at ScienceDirect

Science of the Total Environment

journal homepage: www.elsevier.com/locate/scitotenv

Large spatial variation and stagnation of cropland gross primary production increases the challenges of sustainable grain production and food security in China

Fang Liu [a], Xiangming Xiao [a,*], Yuanwei Qin [a], Huimin Yan [b], Jikun Huang [c], Xiaocui Wu [a], Yao Zhang [d], Zhenhua Zou [e], Russell B. Doughty [f]

[a] Department of Microbiology and Plant Biology, Center for Earth Observation and Modeling, University of Oklahoma, Norman, OK 73019, USA
[b] Institute of Geographic Sciences and Natural Resources Research, Chinese Academy of Sciences, Beijing 100101, China
[c] China Center for Agricultural Policy, School of Advanced Agricultural Sciences, Peking University, Beijing 100087, China
[d] Climate and Ecosystem Sciences Division, Lawrence Berkeley National Laboratory, Berkeley, CA 94720, USA
[e] Department of Geographical Sciences, University of Maryland, MD 20742, USA
[f] Division of Geological and Planetary Sciences, California Institute of Technology, Pasadena, CA 91125, USA

HIGHLIGHTS

- Croplands with continuous increase of GPP were largely distributed in northern China.
- Inconsistent relationship between CGP and GPP before and after 2008
- Grain exporters with limited water storage faced increasing water scarcity.
- Stagnant GPP and rising water scarcity make food security more challenging.
- Sustainable management of land and water resources is highlighted.

GRAPHICAL ABSTRACT

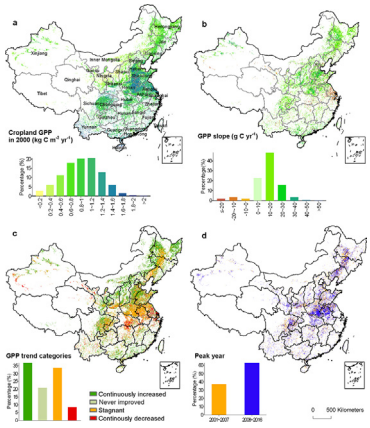

ARTICLE INFO

Article history:
Received 22 July 2021
Received in revised form 29 October 2021
Accepted 30 October 2021
Available online 4 November 2021

Editor: Jay Gan

Keywords:
Cropland productivity
Sustainable agriculture
Water resource storage
Remote sensing

ABSTRACT

Sustainable crop grain production and food security is a grand societal challenge. Substantial investments in China's agriculture have been made in the past decades, but our knowledge on cropland gross primary production in China remains limited. Here we analyzed gross primary production (GPP), solar-induced chlorophyll fluorescence (SIF), terrestrial water storage, crop grain production, and agricultural investment and policy during 2000–2018. We found that based on croplands in 2000, approximately 52×10^6 ha (~37%) had continuous increasing trends in GPP during 2000–2018, which were mainly located in northern China. GPP for 63% of croplands was stagnant, declined, or had no significant change. At the national scale, annual cropland GPP increased during 2000–2008 but became stagnant in 2009–2018, which was inconsistent with the interannual trend in the crop grain production data for 2009–2018. The spatial mismatch between crop production and water availability became worse. The major grain exporting provinces, mostly located in water-stressed regions, experienced increased water resource constraints, which posed a challenge for sustainable grain production. The stagnant cropland GPP and increasing water resource constraints highlight the urgent need for sustainable management for crop production and food security in China.

* Corresponding author.
E-mail address: xiangming.xiao@ou.edu (X. Xiao).

https://doi.org/10.1016/j.scitotenv.2021.151408
0048-9697/

1. Introduction

Crop grain production, food self-sufficiency, and food security in China have substantial impacts on the world's food markets and have been major concerns over the past decades (Brown, 1995; Fukase and Martin, 2016; Gong, 2011). Several factors are well documented, including continued population increases (e.g., 1.27 billion in 2000 to 1.40 billion in 2018) (NBS, 2001–2019), dietary changes among consumers (Lu et al., 2015), limited natural resources, and adverse environmental impacts (Aeschbach-Hertig and Gleeson, 2012; X.P. Chen et al., 2014). In the past decades, several large investments in agriculture have been made in China (Huang and Yang, 2017). For example, about $630 billion USD was invested in water conservation between 2012 and 2020.

The National Bureau of Statistics of China (NBS) compiles and releases crop grain production (CGP) data in China at national and provincial scales. According to the crop grain production dataset from the NBS at the national scale, crop grain production increased continuously over 2003–2014, with a net increase of ~41% between 2014 and 2003 (Jiao et al., 2016), which may be driven in part by improving crop yields (Ray et al., 2012; Wei et al., 2015). The NBS CGP statistical data at provincial and national scales are generated from reports at the county scale and a limited number of field surveys, and they do have considerable uncertainty (Gale et al., 2005; Liu et al., 2020). As the NBS CGP data are used for developing crop grain production and nutrition policies at the national level, their large uncertainty and inaccuracy could potentially have negative impacts on the decision making and national policies and adversely affect food security in China and the world. Crop grain production data at the household level were collected by farm surveys and analyzed in local regions (Yan et al., 2015). As the sample sizes from both the NBS and household survey data are relatively small, the large spatial heterogeneity of croplands in China clearly and strongly raise the need for additional evidence to corroborate the NBS CGP statistical data, so that the effectiveness of large agricultural investment can be assessed accurately and that agriculture-related policies can be appropriately made based on accurate information on the interannual variation and trends of crop grain production.

Cropland gross primary production (GPP) can be estimated using satellite-based remote sensing data, climate data, and data-driven models (Running et al., 2004; Zhang et al., 2017). GPP data have been used to estimate crop net primary production (NPP) (Yan et al., 2016), aboveground biomass (Bastiaanssen and Ali, 2003; Lobell et al., 2003), crop grain production, and crop yield (Burke and Lobell, 2017; He et al., 2018; Reeves et al., 2005; Wu et al., 2021a). The GPP data products (GPP_{VPM}) from the satellite-based Vegetation Photosynthesis Model (VPM) have been evaluated and are highly consistent with GPP data from CO_2 eddy flux tower sites (GPP_{EC}) for maize, soybean, winter wheat, rice, and sugarcane (Wang et al., 2010; Xin et al., 2020; Xin et al., 2017; Yan et al., 2009; Zhang et al., 2016, 2017). The global GPP_{VPM} data during 2000–2016 at moderate spatial resolution (500-m) have been released and evaluated with in-situ GPP data from the FLUXNET sites and solar-induced chlorophyll fluorescence (SIF) data (Chang et al., 2019; Cui et al., 2017; Doughty et al., 2021a; Ma et al., 2018; Wagle et al., 2016; Wu et al., 2018; Zhang et al., 2016). Recently, GPP_{VPM} data were used to study the spatial distribution and temporal dynamics of GPP and grain production for paddy rice in Northeast China during 2010–2017 (Xin et al., 2019) and winter wheat, maize, and soybean in the conterminous United States (CONUS) during 2008–2018 (Wu et al., 2021a; Wu et al., 2021b). The availability of both GPP_{VPM} and the NBS crop statistics offers an opportunity to assess the spatial-temporal consistency between cropland GPP and CGP at national and provincial scales. The availability of GPP_{VPM} data also offers an opportunity to evaluate the effectiveness of various Chinese government investments on cropland GPP since 2000, our findings could help future agricultural development, policies, and investment.

Here, we used cropland GPP data from the VPM (Zhang et al., 2017) at the pixel (500-m), provincial, and national scales and CGP data from the NBS at national and provincial scales during 2000–2018 to investigate the spatial-temporal changes of cropland GPP and CGP in China. First, we investigated the spatio-temporal dynamics of cropland GPP during 2000–2018 at the pixel scale. We found four types of interannual changes in GPP for individual pixels during 2000–2018: (1) a continuous increase trend; (2) stagnant: an increase during the early years that became stagnant during the later years; (3) no significant change; and (4) a continuous decrease trend. We hypothesized that significant areas of croplands in China would have a continuously increasing trend in GPP during 2000–2018 because of the large agricultural investments that were made since 2000. We collected several socio-economic datasets and used them to assess the effectiveness of these agricultural investments on the spatial-temporal dynamics of cropland GPP. Second, we studied the trade-off between cropland GPP and water resource conservation in China during 2002–2016. Finally, we investigated the interannual trends and temporal consistency between cropland GPP data and CGP data in China during 2000–2018 at the national and provincial scales. Our hypothesis was that the interannual variations and trends in cropland GPP would agree well with those of CGP. The results from this study provide new insights into cropland GPP and CGP in China during 2000–2018, which have important impacts on assessing food security.

2. Materials and methods

2.1. Remotely sensed data

2.1.1. Cropland data

The cropland data was derived from the China National Land Cover Datasets (NLCD-China) (Liu et al., 2005). First, land cover vector maps (cropland, forest, grassland, water body, built-up land, and unused land) were produced through visual interpretation and digitization of 512 Landsat ETM+ images. The accuracy assessment of the dataset was carried out through the extensive field survey dataset, and the cropland data layer in 2000 had an overall accuracy of 94.9%. Second, the cropland vector map was overlaid with 1-km grid cells to generate raster cropland data with the area fraction of cropland for each grid cell (% cropland). In this study, due to the data availability, the 1-km raster cropland dataset in 2000 was used as the baseline for the data analyses. The cropland data used in our study was freely provided by the Resources and Environmental Science Data Center of the Chinese Academy of Sciences (Xu et al., 2018). According to the previous studies that used the NLCD-China, the total cropland area decreased by 1% in 2000–2015 (Liu et al., 2014; Ning et al., 2018), which suggested that the cropland area was relatively stable.

2.1.2. Cropland gross primary production (GPP) data

We used the VPM GPP dataset at a 500-m spatial resolution and 8-day temporal resolution during 2000–2018 (Xiao et al., 2004a,b; Zhang et al., 2017). The input datasets for the VPM simulations include the Moderate Resolution Imaging Spectroradiometer (MODIS) 8-day, 500-m surface reflectance product (MOD09A1 C6), the 8-day, 1-km land surface temperature product (MYD11A2 C5), the land cover product (MCD12A2 C5), and the downward shortwave radiation and air temperature from the NCEP-DOE Reanalysis 2 dataset (Zhang et al., 2017). The 8-day GPP data were aggregated into annual GPP values (g $C\ m^{-2}\ yr^{-1}$) for inter-annual analysis. The annual GPP datasets were aggregated from 500-m spatial resolution to 1-km spatial resolution using the weighted average method to be consistent with the cropland layer. Then, the annual total GPP of cropland (g $C\ yr^{-1}$) at 1-km spatial resolution was calculated as the product of annual GPP (g $C\ m^{-2}\ yr^{-1}$) and the total cropland area from the NLCD-China dataset, and the resultant annual total cropland GPP was further summed to 0.5 degree (latitude and longitude) at the provincial and national scales.

2.1.3. Solar-induced chlorophyll fluorescence (SIF) data from GOME-2

SIF is energy emitted by plant leaves after its chlorophyll pigment absorbs photosynthetically active radiation. The monthly GOME-2 SIF dataset (Version 27) has a spatial resolution of 0.5 degree, which was retrieved using a principal component analysis approach at wavelengths around 740 nm with ~0.5 nm spectral resolution. Compared to GOME-2 SIF (Version 26), GOME-2 SIF (Version 27) had new post-processing of retrievals, which provided additional fields and improved bias corrections and calibration (Joiner et al., 2013, 2016; Joiner et al., 2014). The comparisons between the GOME-2 SIF and GPP_{VPM} products have shown that they have high spatio-temporal consistency in North America in 2010 (Zhang et al., 2016), one maize site in the United States during 2007–2011 (Wagle et al., 2016), ten megacities during 2007–2014 (Cui et al., 2017), China during 2007–2014 (Ma et al., 2018), evergreen forest and deciduous forest in the northern hemisphere during 2007–2016 (Chang et al., 2019), the contiguous United States (CONUS) during 2008–2014 (Wu et al., 2018), and in the Amazon basin (Doughty et al., 2021b). We calculated the annual average SIF using the monthly SIF values after excluding the grid cells without SIF values.

2.1.4. Terrestrial water storage (TWS) data

TWS includes vegetation water, soil water, surface water, groundwater, snow, and ice (Girotto et al., 2016). Its seasonal and interannual variations provide critical information for assessing regional water resource deficit or water availability (Jing et al., 2019; Scanlon et al., 2018). GRACE satellites provide estimates of TWS over time, which help address the impacts of both climate and human activities on TWS (Zhao et al., 2020). TWS data during 2002–2016 was used because of the data gap between the GRACE mission (ended in October 2017) and GRACE Follow-On mission (from June 2018). The data was derived from the GRACE liquid water-equivalent thickness (LWET) data (Wiese, 2015). The monthly LWET data at a spatial resolution of 0.5° provided the anomalies relative to the 2004.0–2009.999 time-mean baseline. After applying the mascon-set of 0.5-degree gain factors to reduce leakage errors (Wiese et al., 2016), the monthly LWET data was aggregated to annual average values (Zou et al., 2018).

2.1.5. Digital Elevation Model (DEM)

The 1-km DEM was used in this study acquired from the Shuttle Radar Topography Mission (SRTM). The slope and the terrain relief index, defined as the maximum height difference in a window of 5 km × 5 km, were calculated in ArcGIS 10.4 software.

2.2. Socio-economic data

2.2.1. Crop grain production (CGP) data

The National Statistical Bureau of China (NBS) releases the annual China Statistical Yearbook, which contains the national-scale data for all the prior years and provincial-scale data for the previous year. The national annual CGP data during 2000–2018 was collected from the China statistical yearbook in 2019. The provincial annual CGP was derived from the China statistical yearbooks for 2001–2017. CGP in this study includes the production of major grain crops (wheat, rice, maize, and soybean) grown in China. Annual CGP data at the national and provincial scales during 2000–2018 was used for the trend and consistency analyses with cropland GPP.

2.2.2. Agricultural investment and policy data

Annual data for indicators of agricultural investment and policy at the national scale were collected during 2000–2018. The annual crop planted area, irrigated cropland area, fertilizer use, agricultural tax, and government investment in agriculture were collected from the China statistical yearbook (2001–2019). Annual price data for major grain crops were collected from the Compilation of National Farm Product Cost-Benefit Data (2001–2017). Annual agricultural subsidy data came from the previous study (Huang and Yang, 2017) and an update by Huang's group. The agricultural subsidy program included grain price subsidy, input subsidy, quality seed subsidy, and agricultural machinery subsidy. The agricultural subsidy program became a direct-payment subsidy program to farmers in 2004 and gradually increased until 2012. After 2016, the agricultural subsidy program was further improved by allocating 20% of the funds from the aggregate input subsidy to support farmland management. The subsidy payment of grain price subsidy and input subsidy went directly to farmers, which increases the farmers' income.

2.2.3. Population data

Annual population data at the national and provincial scales were collected from the China statistical yearbooks (2001–2019).

2.3. Statistical analyses for interannual trends of GPP and CGP during 2000–2018

A simple linear regression model was used to quantify the interannual trends of cropland GPP and CGP during 2000–2018. To explore the trajectory of GPP and CGP trends over time, we further reclassified the interannual trends of GPP and CGP into four types. The procedure includes three steps. First, GPP or CGP time series data for individual provinces or pixels were fitted using three statistical models (an intercept-only model, linear model, and quadratic model) at the provincial and pixel scales (Table 1 and Fig. 1) and then determined the best fit models based on the minimum Akaike Information Criterion (AIC) (Akaike, 1981). Second, the goodness of the chosen models was evaluated before using the models to identify and label specific types of interannual trends. The test was conducted using F statistic against the null hypothesis of a constant model. Third, the interannual trends of GPP and CGP were classified according to the parameters of the chosen models (Table 1). Following the classification method for interannual trends (Ray et al., 2012), interannual trends of GPP and CGP during 2000–2018 at the scales of pixel (GPP only) and province (both GPP and CGP) were classified into four types: (1) continuous increase (positive slope with p-value < 0.05); (2) no significant change (positive or negative slope with p-value ≥ 0.05); (3) continuous decrease (negative slope with p-value < 0.05, and (4) stagnant (best fitted using quadratic model (p-value < 0.05) with negative quadratic term and peak year before 2018), whereby GPP or CGP increased in the early years (e.g., 2000s) but become stagnant in later years (e.g., 2010s). Table 1 provided the detailed procedure for classification of the trends. Illustrative examples of the four classifications of GPP interannual trends were shown in Fig. 1. The turn-point year (the year after peak year for stagnant trend) was defined as the point where mean and the slope of the GPP change most abruptly. The turn-point year was detected based on time series GPP and CGP data using the findchangepts function (Killick et al., 2012) in MATLAB 2017b.

2.4. Statistical analyses for the relationships among GPP, CGP, and driving factors

We explored the relationship between GPP and CGP in two ways. First, the relationships between cropland GPP and CGP during the entire period (2000–2018) at the national and provincial scales were quantified using the linear regression models (CGP = f(GPP)), including F-statistic, slope value, and significance level. Second, we classified the trends in GPP and CGP separately and compared the different types of trends between GPP and CGP at both national and provincial scales.

The relationships between cropland GPP and GRACE TWS were analyzed in two steps. First, linear regression was used for the interannual trend analysis of GRACE and GPP (0.5 degree), and the geographical distributions of those grid cells with significant trends of GRACE and GPP (p-value < 0.05) were identified and mapped by overlaying these two trends. Second, a simple linear regression model was used to quantify

Table 1
Decision trees for four types of interannual trends of cropland gross primary production (GPP) and crop grain production (CGP) at provincial and pixel scales during 2000–2018.

Regression models	Criteria	Best fit models				Categories
$y = ax^2 + bx + c$	*Minimum AIC*	$y = ax^2 + bx + c$	$p \geq 0.05$			No significant change
$y = mx + n$			$p < 0.05$	$a > 0$	$\frac{-b}{2a}$<2018	Continuous increase
$y = k$					$\frac{-b}{2a}$≥2018	Continuous decrease
				$a < 0$	$\frac{-b}{2a}$<2009	Continuous decrease
					2009≤$\frac{-b}{2a}$<2018	Stagnant
					$\frac{-b}{2a}$≥2018	Continuous increase
		$y = mx + n$	$p \geq 0.05$			No significant change
			$p < 0.05$	$m > 0$		Continuous increase
				$m < 0$		Continuous decrease
		$y = k$	$p \geq 0.05$			No significant change
			$p < 0.05$			No significant change

the relationship between annual cropland GPP and GRACE TWS with *t*-tests at the 5% significance level at individual grid cells.

3. Results and discussion

3.1. Spatio-temporal dynamics of cropland GPP during 2000–2018 at pixel scale

At the pixel scale (a total of 1841,497 pixels), cropland GPP (g C/m^2/yr^{-1}) in 2000 had large spatial variations across the country (Fig. 2a), and 70% of the cropland pixels ranged between 0.6 kg C m^{-2} yr^{-1} and 1.4 kg C m^{-2} yr^{-1} (Fig. 2a). The simple linear regression model (GPP = f(year)) showed that the interannual trends (slope) of GPP during 2000–2018 also had large spatial variation (Fig. 2b). Approximately 60% of the cropland pixels had significant (*p*-value < 0.05) increases in GPP during 2000–2018, most of which were in northern China (Fig. 2b). Approximately 5% of the cropland pixels had significant (p-value < 0.05) decreases in GPP, which were mainly in the Lower Yangtze Plain (Shanghai, Jiangsu, and Zhejiang), where urbanization quickly replaced high-quality croplands (Liu et al., 2014).

The interannual trends of GPP during 2000–2018 at individual cropland pixels were further classified into four types of trajectory (Fig. 2c), and each of these four trajectories were due to many factors. Approximately 37% of the cropland pixels were "continuous increase of GPP", mostly in the Northern China Plain. In order to increase crop yield (ton/ha), the Chinese government carried out various projects that provided substantial financial investment, policy support, and resource inputs (e.g., water, fertilizer, and machinery) to agriculture, which were considered to be the major driving factors for the large increases of crop yield and CGP in China (Huang and Yang, 2017; Li et al., 2014). As the gross domestic product (GDP) increased, government financial investments in agriculture increased gradually during 2000–2008 and then rose substantially during 2009–2016 (Fig. 3a). In an effort to address food security and rising income gaps between rural and urban people, a direct-payment subsidy program to farmers was first implemented in 2004 and the amount of money gradually increased until 2012 (Fig. 3b), which had moderate impacts on CGP and farmer incomes (Huang et al., 2011; Huang and Yang, 2017). In 2016, the subsidy program was further improved by allocating 20% of the funds from the aggregate input subsidy to support farmland management. The

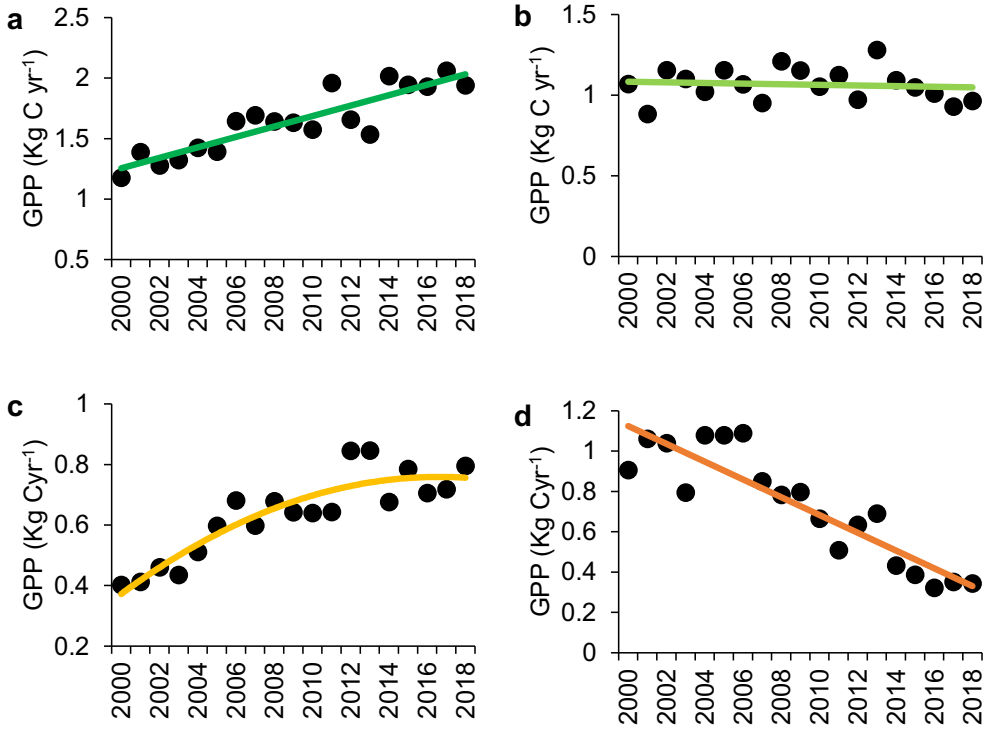

Fig. 1. Examples of four categories of GPP interannual trends for four pixels (1-km spatial resolution). (a) Continuous increase (116.498E, 37.0751N), (b) no significant change (105.3774E, 30.4578N), (c) stagnant (106.293E, 34.7513N), and (d) continuous decrease (120.162E, 33.0158N).

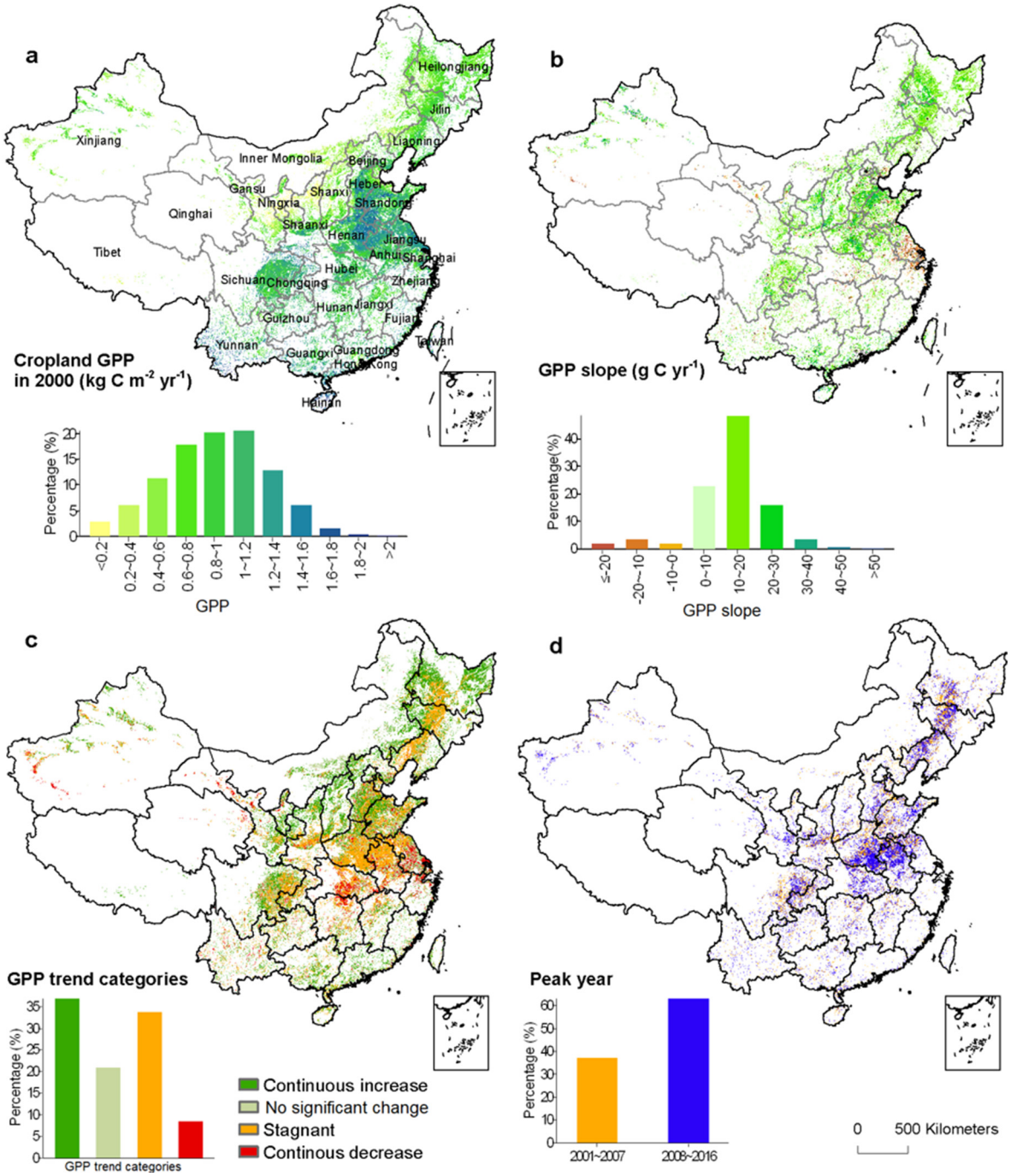

Fig. 2. The spatial distribution and interannual trend of cropland GPP during 2000–2018. (a) Annual cropland GPP in 2000. (b) Interannual trend (slope value) of annual cropland GPP ($P < 0.05$) during 2000–2018. (c) Four categories of interannual trends of annual cropland GPP during 2000–2018. (d) The peak year of GPP stagnation.

agricultural tax was high in 2002–2003 and was abolished in 2006 (Fig. 3b). The market prices of major crops increased substantially in 2004 and 2010 (Fig. 3c), which was primarily driven by a guaranteed limit purchase price policy and a temporary purchase and storage policy to ensure farmers' income and enthusiasm for crop cultivation (Huang and Yang, 2017). Irrigation and fertilizer use increased crop yields (Guo et al., 2010; H.Y. Wang et al., 2017). Irrigated cropland area in China increased from 53.82 million ha in 2000 to 68.27 million ha in 2018, an increase of 27% (Fig. 3d). The use of fertilizers (N, P, K, and compound fertilizer) in China increased gradually from 41.46 million tons in 2000 to 56.53 million tons in 2018, an increase of 36.35% (Fig. 3e).

Approximately 8% of the cropland pixels were "continuous decrease" in term of GPP trajectory, mostly in Hubei and Jiangsu Provinces. Urbanization, industrialization, and infrastructure construction in China have resulted in a loss (−0.7%) of the total cropland area in 2000–2015 (Liu et al., 2014; Ning et al., 2018). Approximately 21% of the cropland pixels were "no significant change", which were mostly in Jiangsu and Sichuan. Approximately 34% of the cropland pixels were "stagnant (increased GPP during the early years but became stagnant in later years)", which were mostly in Henan, Jiangsu, Anhui, and Liaoning Provinces. The peak years before cropland GPP became stagnant varied across the country (Fig. 2d). Out of those cropland areas with stagnant GPP, ~37% became stagnant before 2009, mostly in southern China, and ~63% became stagnant in or after 2009 and were concentrated in the grain production provinces (Fig. 2d).

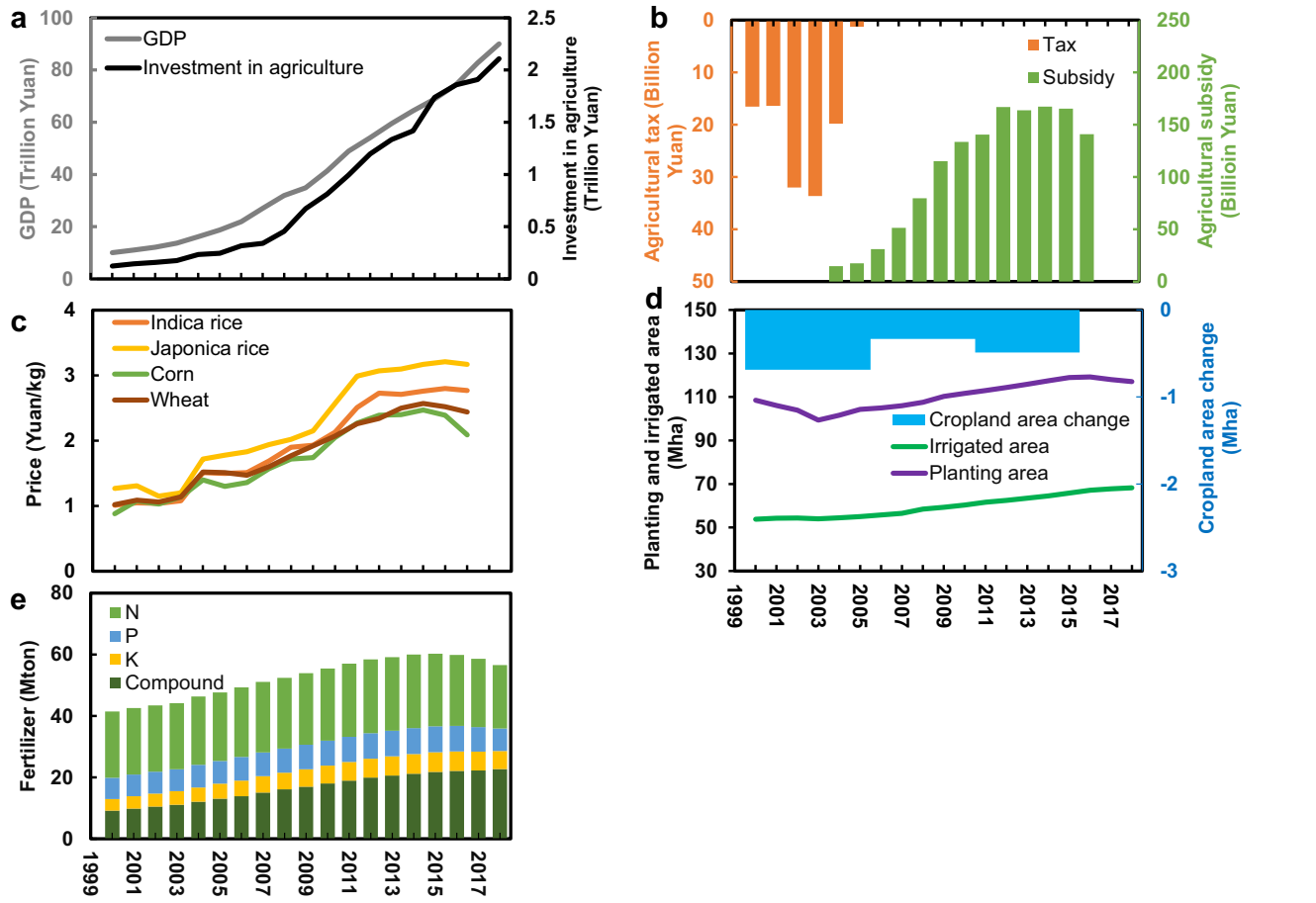

Fig. 3. Interannual variations of agriculture policy and economic indicators and crop trade in China during 2000–2018. (a) Gross domestic product (GDP) and investment in agriculture during 2000–2018. (b) Agricultural tax and subsidies data during 2000–2016. (c) Major crop purchase price during 2000–2016. (d) Changes in cropland area (2000–2005, 2005–2010, and 2010–2015), planting area, and irrigated area (2000–2018). (e) Fertilizer application during 2000–2018, including nitrogen (N), phosphorus (P), potassium (K), and compound fertilizer.

Many cropland pixels already had high production in early 2000s, reaching 70–80% of potential yield, thus they could become stagnant in late 2000s because of its difficulty to raise yields (Cassman et al., 2003; Grassini et al., 2013; van Ittersum et al., 2013). Decreasing cropping intensity (numbers of crops per year in a crop field) in southern China may lead to GPP decrease or stagnation. Many croplands with double-cropping systems in early 2000s were converted to single-cropping systems due to lack of farm workers and/or small income from crop grain sale (Yan et al., 2019). The rising cost and small income for major grain crops after 2008 reduced farmers' enthusiasm for crop production (Yan et al., 2019). The net revenue for farmers is low due to the rising cost of crop cultivation. For example, the rural labor wages increased by 8% annually after the mid-2000s (Huang and Yang, 2017; Li et al., 2013). Inappropriate use of chemical fertilizers and irrigation in some croplands led to soil degradation and decline of crop yields (Huang and Rozelle, 1995; Kuang et al., 2021; Rozelle et al., 1997). Beginning in 2011, a high priority for China was to improve crop yield by implementing “high-standard cropland” projects, which aimed to cover 20% of the total cropland area by 2015 and 40% of the total cropland area by 2020, respectively. The remaining cropland areas may not receive sufficient resources to maintain or improve their productivity in those years (Huang and Yang, 2017; Ray et al., 2012; Wei et al., 2015).

3.2. Trade-off between cropland GPP and water resource conservation during 2002–2016

Irrigation is one of the major factors that affect the interannual trends of cropland GPP in China, and currently about 50% of croplands in China are irrigated (Huang and Yang, 2017). The large increase of irrigated cropland area in China during 2000–2016 (Fig. 3d) was achieved by the government's substantial investment in water resource infrastructure and irrigation from surface water and groundwater (Du et al., 2019), which is reflected in the temporal changes of TWS over years in China. The relationships between cropland GPP and TWS during 2002–2016 at the grid cell and provincial scales were investigated to seek new insights on the limit and potential of water sources for cropland GPP and CGP in China (Figs. 4 and 5).

At the scale of grid cells (0.5°), the spatial distributions of the interannual trends of cropland GPP and GRACE TWS during 2002–2016 (Fig. 4a, b) show the hot-spot areas with significant interannual changes in GPP and TWS. Out of 3833 grid cells with croplands, GRACE TWS decreased significantly ($P < 0.05$) in 1557 grid cells (35%) and increased significantly ($P < 0.05$) in 1282 grid cells (33%) (Fig. 4b). The temporal consistency in the interannual trends of cropland GPP and GRACE TWS was further evaluated (Fig. 4c). Six hundred grid cells (24%) had a significant ($P < 0.05$) positive trend in cropland GPP but a negative trend in GRACE TWS, mostly in the North China Plain. Although the North China Plain is under high water stress, a high irrigation rate (66% in 2015), increased cropping intensity (single to double cropping), and increased field sizes (2000–2015) (Yan et al., 2019) fueled crop production. Four hundred and eighty-five grid cells (18%) had significant ($P < 0.05$) increases in both cropland GPP and GRACE TWS (Fig. 4c), mostly in Northeast China and South China. The simple linear regression analysis showed that 273 grid cells (8%) had a significant ($P < 0.05$) positive linear relationship between cropland GPP and GRACE TWS while 467 grid cells (17%) had a significant ($P < 0.05$) negative linear relationship (Fig. 4d).

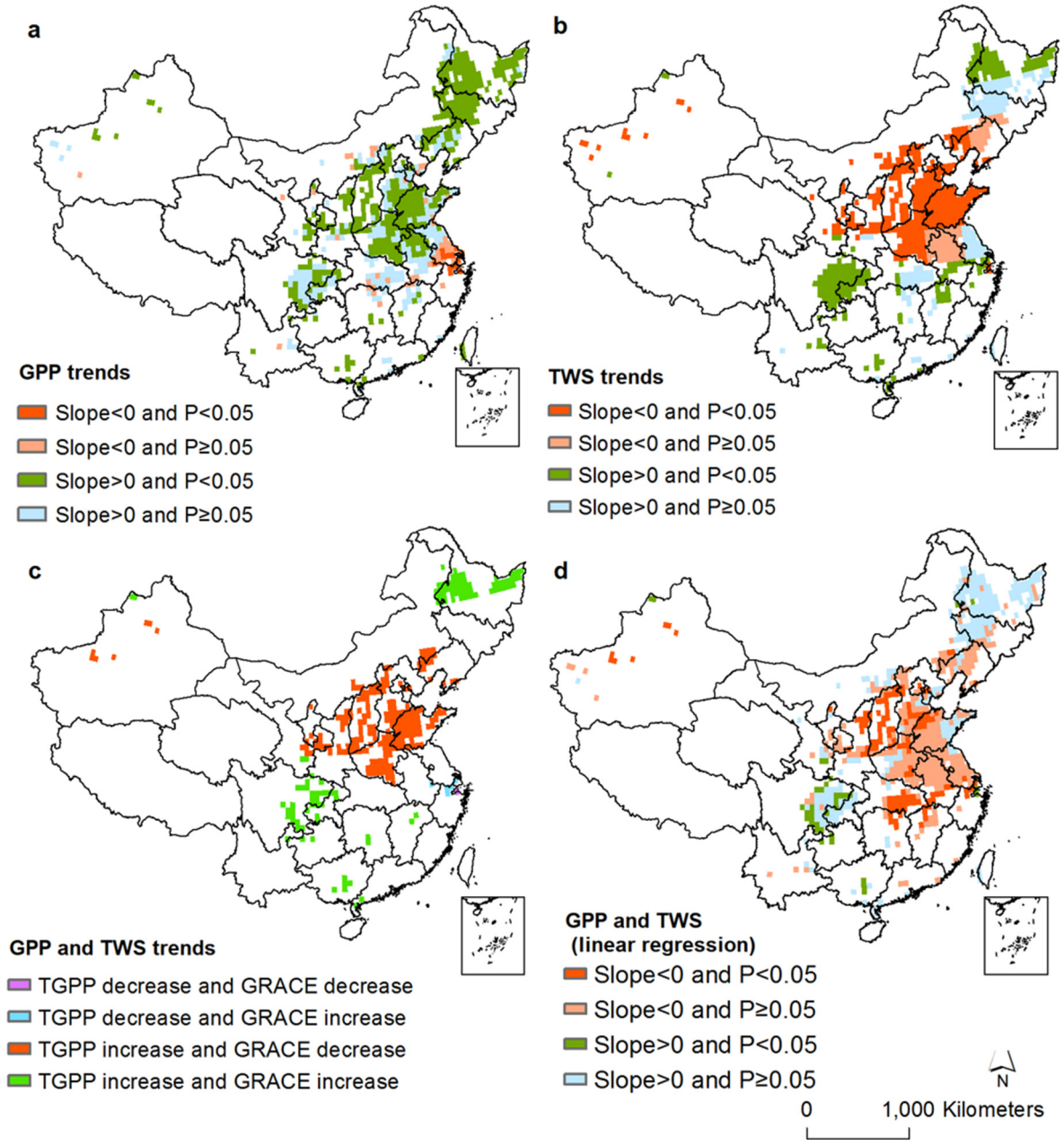

Fig. 4. The relationships between cropland GPP and the terrestrial water storage (TWS) during 2002–2016 in China at individual grid cells (0.5° spatial resolution) with *t*-tests at the 5% significance level. (a) Interannual trends of cropland GPP (unit: Tg C yr^{-1}). (b) Interannual trend of GRACE TWS (unit: cm). (c) Relationships between GRACE TWS trends and cropland GPP trends for those grid cells with $P < 0.05$ in (a) and (b). (d) Slope and *P* values of linear regression models between annual cropland GPP and GRACE TWS at individual grid cells. Cropland map at the 0.5° × 0.5° spatial resolution was aggregated from the NLCD-China cropland map at 1 km spatial resolution and contains the area percentage of cropland within each grid cell.

At the provincial scale, the temporal changes of GRACE TWS during 2002–2016 (Supplemental Fig. 1) showed that ten provinces had significant ($P < 0.05$) negative trends in GRACE TWS, most of them located in regions with limited water resources, such as the North China Plain (Hebei, Shandong, and Henan), the Loess Plateau (Shanxi, Ningxia, Gansu), and Xinjiang. Ten provinces had significant ($P < 0.05$) positive trends in GRACE TWS, most of which were in regions with abundant water resources, such as South China (Sichuan, Chongqing, Fujian, Jiangxi, and Hainan) (Supplemental Fig. 1). The temporal consistency between annual GPP and GRACE TWS during 2002–2016 varied by province (Fig. 5). The major grain exporting provinces, mostly located in water-stressed regions with irrigated agriculture, experienced losses in GRACE TWS. In Hebei, Henan, and Shandong Provinces, GRACE TWS dropped substantially after 2004, while cropland GPP was stagnant (Fig. 5a, b, c). These provinces had larges areas of winter wheat and summer maize crops, and irrigation of these crop fields (Siebert et al., 2010) had consumed large amounts of water (Wang et al., 2008), including groundwater (Aeschbach-Hertig and Gleeson, 2012). For example, the groundwater table declined by 1 m per year in Hebei during 2000–2014 (Yang et al., 2015). In Xinjiang Province, GRACE TWS continuously decreased while cropland GPP increased gradually (Fig. 5e). In Heilongjiang Province, both GRACE TWS and cropland GPP increased (Fig. 5g) due to the substantial rice paddy expansion (Zhang et al., 2020). In addition to the rising demand by the agricultural sector for water, the rapid population growth, industrialization, and urbanization also increased domestic and industrial demands for water resources. Beijing, Shanghai, and Tianjin had large losses in GRACE TWS over the years (Fig. 5m, n, o).

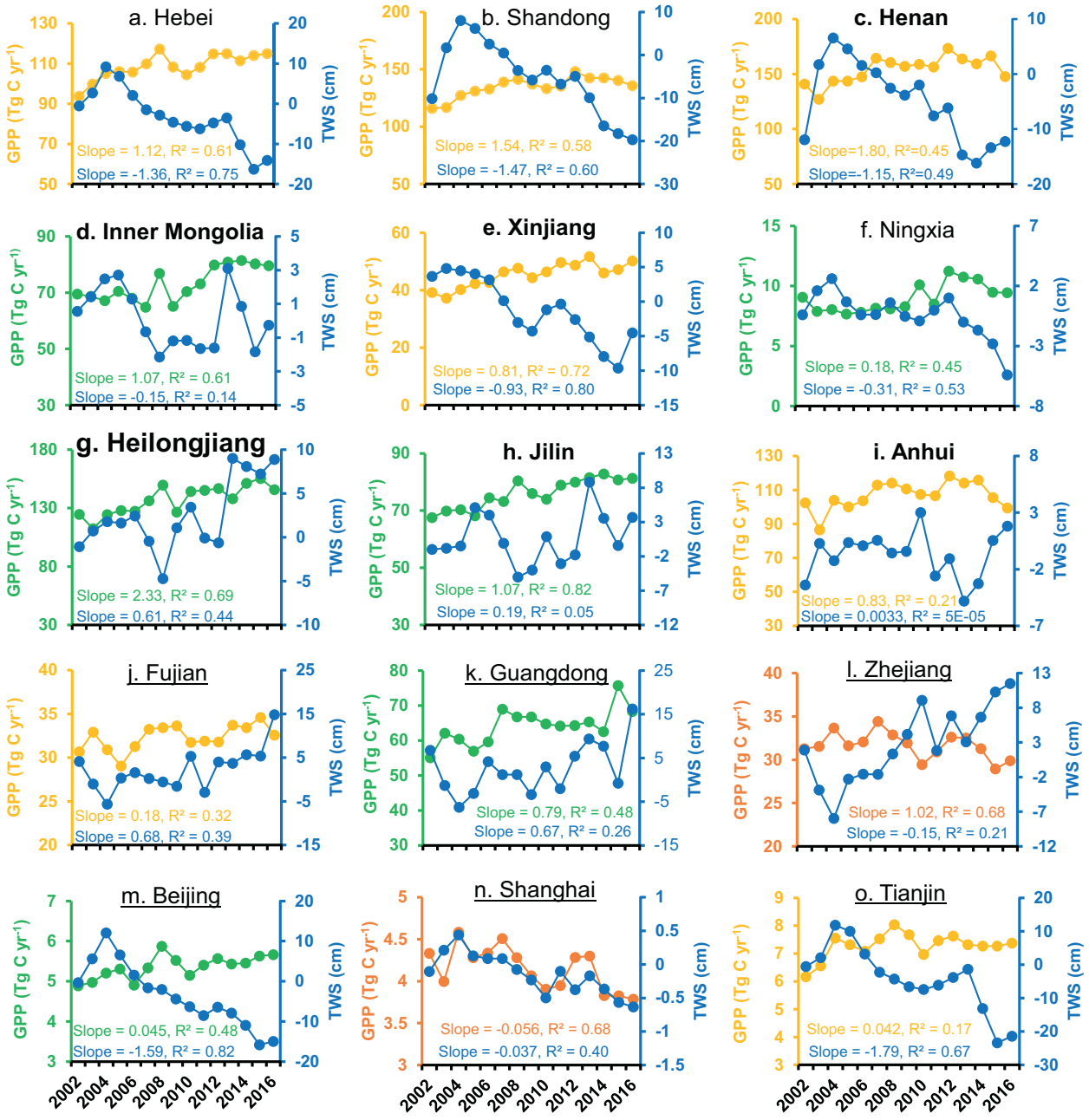

Fig. 5. Interannual variations of annual GPP and GRACE TWS of croplands at the provincial scale during 2002–2016. Grain-exporting and importing provinces were determined by comparisons between CGP per capita at the provincial scale and national CGP per capita. Top six grain exporters (Henan (c), Inner Mongolia (d), Xinjiang (e), Heilongjiang (g), Jilin (h), and Anhui (i) Provinces) and grain importers (Fujian (j), Guangdong (k), Zhejiang (l), Beijing (m), Shanghai (n), and Tianjin (o)) are highlighted using bold and underline, respectively. The colors of the annual GPP mean the four categories of GPP trends, as shown in Fig. 1.

Irrigated agriculture has been threatened by increasing water scarcity (J. Wang et al., 2017). Many previous studies have reported groundwater depletion in various regions in China, which severely affects CGP (Aeschbach-Hertig and Gleeson, 2012; Siebert et al., 2010; Yang et al., 2015). Compared to the irrigated maize in China in the 2000s, the yield of the rainfed maize was ~10% lower and even >20% lower in some areas (Meng et al., 2016). Over the past two decades, water scarcity has resulted in an annual CGP loss of more than 27 million tons in China (H. Chen et al., 2014). Wheat production in the North China Plain is most threatened by water scarcity, and the introduction of irrigation systems has driven large increases in CGP and severe groundwater depletion in this region over the last 40 years (Dalin et al., 2017; Gale et al., 2005). Because surface water supplies are not reliable, many farmers who do not have secure access to groundwater have abandoned wheat cultivation (Gale et al., 2005). Previous studies also reported the spatial mismatch between croplands and water resources in China (Dalin et al., 2014). The net grain transfer increased from 10 million ton in 2000 to 83 million ton (~13% of the total CGP) in 2013 from north China (poor water resources) to south China (rich water resources) (Jiang et al., 2017). We found that the spatial mismatch between croplands and water resources worsened during 2002–2016, which highlights the constraints of water resources on cropland GPP and CGP in China. Irrigation water use in the North China Plain was ~2 times more than in the High Plains of the United States, but the average crop yield in the North China Plains was only 15% higher than that in the High Plains (Pei et al., 2015). Given the essential role of irrigation (Zhu et al., 2013), to raise agricultural water use efficiency and prevent further loss of groundwater has been and will continue to be the major

challenge for the sustainability of irrigation, water resources, and agriculture in China (Jagermeyr et al., 2016; MacDonald et al., 2016).

3.3. Stagnant crop production and two contrasting views on food security during 2009–2018

At the national scale, annual CGP in China from the NBS dataset increased linearly from 462.18 million ton in 2000 to 534.34 million ton in 2008 (15.6% increase over the year 2000) and 660.60 million ton in 2015 (23.6% increase over the year 2008) but then became stagnant during 2016–2018 (Fig. 6a). Cropland GPP in China also linearly increased from 1.66 Pg C in 2000 to 2.13 Pg C in 2008, an increase of 28.31% (Fig. 6a). Coincidently with the world economic crisis in 2008/2009, cropland GPP in China dropped in 2009 and then remained stagnant from 2009 to 2018 (~2.10 Pg C) (Fig. 6a). Cropland GPP clearly had two distinct periods: a significant ($P < 0.01$) linear increase in 2000–2008 and a stagnant period in 2009–2018. The relationship between CGP and GPP is statistically significant ($R^2 = 0.79$, $P < 0.01$) in 2000–2008, but not significant ($R^2 = 0.11$, $P = 0.29$) in 2009–2018 (Fig. 6b).

We further investigated the temporal consistency between cropland GPP and CGP at the provincial scale. As the CGP data in 2017–2018 at the provincial scale were not available, we analyzed cropland GPP and CGP data during 2000–2016 at the provincial scale (Fig. 7). Simple linear regression models were used to quantify the temporal relationship between cropland GPP and CGP at the provincial scale. Significant linear relationships ($P < 0.05$) between cropland GPP and CGP were identified in 26 provinces, such as Shanxi, Shaanxi, Shandong, Henan, Hunan, Ningxia, and Gansu (Supplemental Table 1). The trajectory of GPP and CGP trends over time during 2000–2016 varied by province (Fig. 7). We found a strong temporal consistency between GPP and CGP in many provinces, such as Jilin, Liaoning, Heilongjiang, and Shanxi. The large temporal divergence between GPP and CGP also occurred in a few provinces, such as Fujian, Guangdong, and Beijing. The interannual trends of cropland GPP and CGP were grouped into four types (Fig. 7). The CGP's interannual trend was a continuous increase in 21 provinces, no significant change in four provinces, stagnant in two provinces, and a continuous decrease in four provinces (Fig. 7, Supplemental Fig. 2b). In comparison, the interannual trends of cropland GPP was a continuous increase in ten provinces, no significant change in one province, stagnant in 18 provinces, and continuous decrease in two provinces (Fig. 7, Supplemental Fig. 2a).

The large discrepancy of interannual trends between cropland GPP and CGP during 2009–2018 at the national scale (Fig. 6a) leads to two contradictory views on CGP and food security in China. In one view, one can assume the CGP data released by the NBS to be true, and thus there is no major concern about CGP and food security in China during 2009–2018. However, the accuracy of crop statistical data (e.g., cropland area, crop production) from the NBS has been frequently debated (Gale et al., 2005; Liu et al., 2020; Xiao et al., 2003). Note that the CGP data released by the NBS in 2019 (2000–2018) differ from the data released by the NBS in 2017 (2000–2016), with increasing differences after 2008 (Supplemental Fig. 3). The three national agricultural censuses of China occurred in 1996, 2006, and 2016, and the results from the second (2006) and third (2016) national agricultural censuses were used to adjust annual CGP numbers in those NBS reports (Fig. 6a, Supplemental Fig. 3).

In another view, one can assume that the strong linear relationship ($R^2 = 0.79$, $P < 0.01$) between cropland GPP and CGP in 2000–2008 holds true over years (Fig. 2b), and as cropland GPP was stagnant during 2009–2018, we can then claim that CGP in China was likely to be stagnant during 2009–2018, (Fig. 6a). Five other studies support this

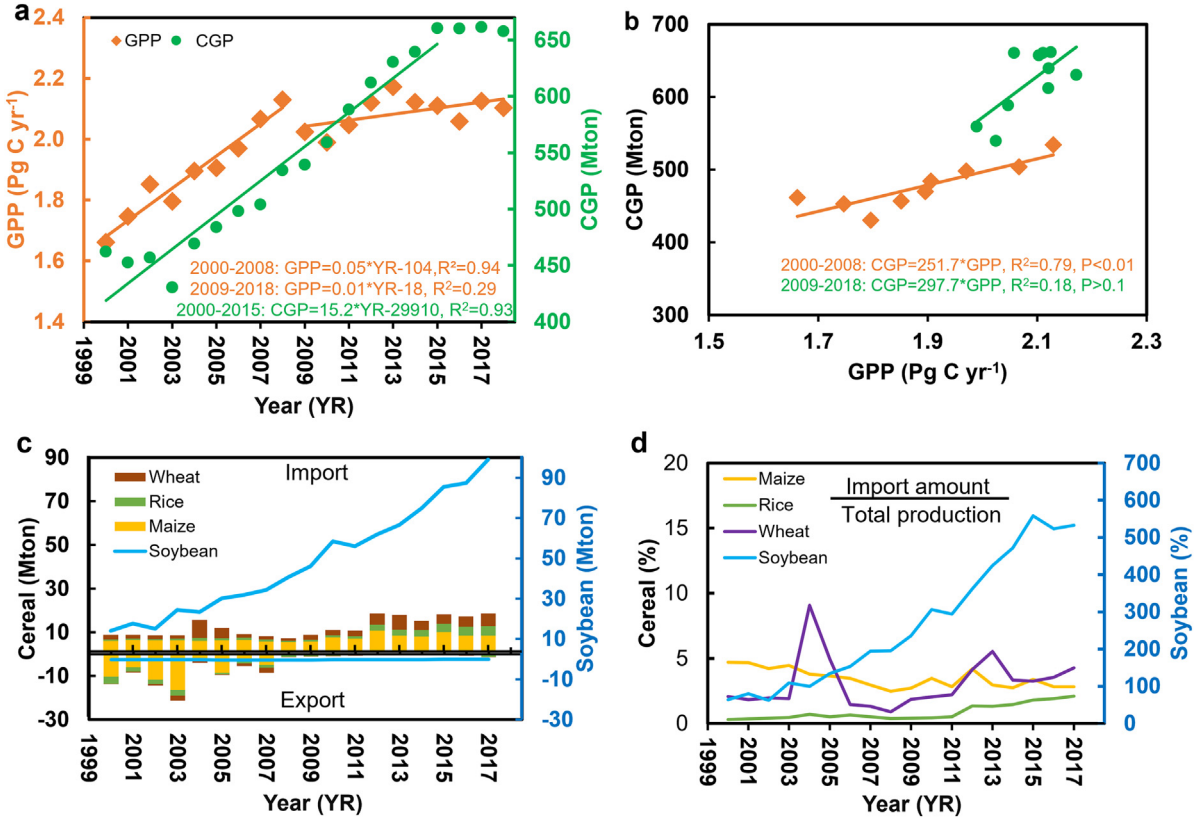

Fig. 6. Interannual variations of cropland gross primary production (GPP), crop grain production (CGP), grain export and import in China during 2000–2018. (a) Linear regressions of GPP (2000–2008; 2009–2018) and CGP (2000–2015). (b) Two-dimension scatterplot between GPP and CGP during 2000–2018 and the linear relationships between GPP and CGP in two periods: 2000–2008 and 2009–2018. (c) Import and export quantity of cereal (maize, rice, and wheat) and soybean during 2000–2017 from FAOSTAT (http://www.fao.org/faostat/en/#data/TP). (d) The ratio between import amount and the total production from China by crop types during 2000–2017.

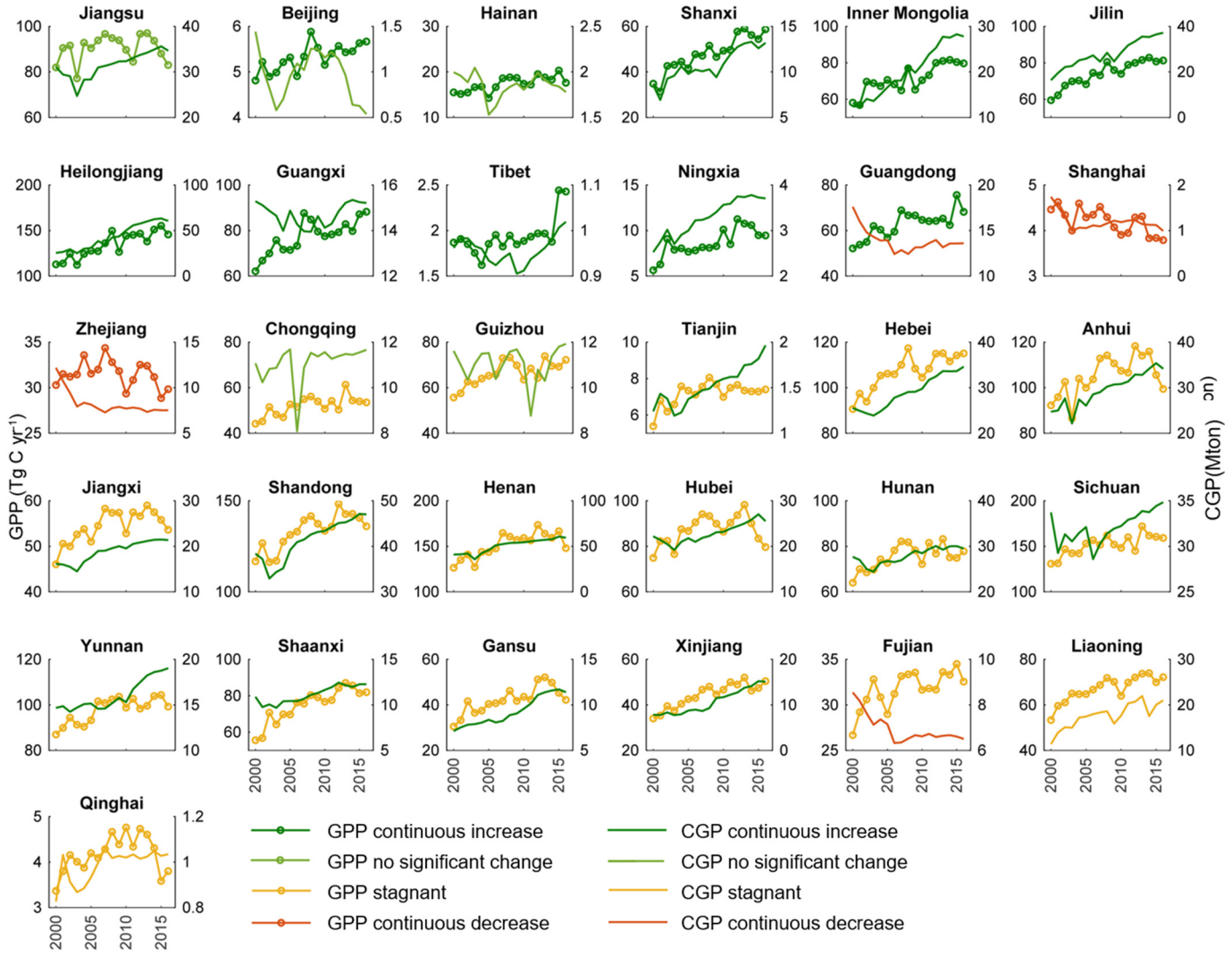

Fig. 7. Interannual variations and trends in cropland gross primary production (GPP) and crop grain production (CGP) at the provincial scale during 2000–2016.

view. First, our cropland GPP data (VPM-based) were evaluated with high consistency with GPP data from 22 eddy flux tower sites for various crop types in a single year or multiple years in China and the globe (Supplemental Table 2). VPM-based GPP of crops (Maize and soybean) has been demonstrated strong linear relationship ($R^2 > 0.9$) with grain production derived from USDA-NASS statistical data (Wu et al., 2021a; Wu et al., 2021b). Second, the spatio-temporal changes of annual GPP were evaluated and had similar trends with the solar-induced chlorophyll fluorescence (SIF) data from the Global Ozone Monitoring Experiment 2 (GOME-2) (Supplemental Table 3). The cropland GPP and GOME-2 SIF data used in this study also had similar trends in the North China Plain (Hebei, Henan, Shandong, Jiangsu, and Anhui) where croplands were dominant, indicating the reliability of stagnant cropland GPP during 2009–2018 in China (Fig. 8). Third, the CGP data during 2009–2016 from the two NBS reports did have large differences (Supplemental Fig. 3). Fourth, crop grain imports rose substantially during the 2010s (Fig. 6c, d). China had imported and exported relatively small amounts of wheat, corn, and rice during 2000–2007, but by 2008 China began to have no exports of these crops (Fig. 6c). China's shift from a country with both crop import and export to a country with only crop import in 2008/2009 coincided with cropland GPP stagnation in 2009. The total amount of imported crops (wheat, corn, rice, and soybean) was 101.50 million ton in 2015 and 102.52 million ton in 2016 (Fig. 6c), which was only moderately lower than the difference (126.26 million ton) in CGP between 2008 (534.34 million ton) and 2015 (660.60 million ton) from the NBS dataset (Fig. 6a). The proportions of imported crops (wheat, corn, and soybean) over the amounts of CGP in China also started to rise in 2009 (Fig. 6c). Finally, several previous studies reported that crop yields in several major grain-producing regions stagnated because average farm yields have reached 70–80% of potential yields (Cassman et al., 2003; Grassini et al., 2013; van Ittersum et al., 2013),

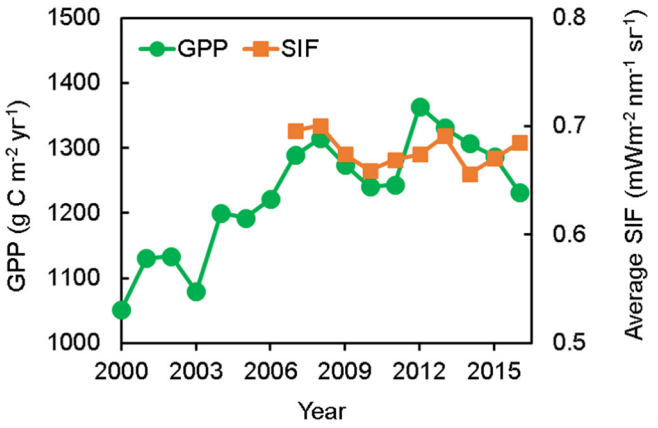

Fig. 8. Comparison between GPP and GOME-2 SIF in the North China Plain, including Hebei, Henan, Shandong, Jiangsu, and Anhui Provinces.

including several rice-producing provinces in China (Hunan, Zhejiang, and Jiangxi Provinces). The cropland area with stagnant GPP also had an average GPP of 1.22 kg C m^{-2} yr^{-1}, which was about 15–22% higher than the average GPP in other cropland areas. Based on our analyses, the NBS crop grain production statistical data after 2008 might have noticeable uncertainties. Therefore, there is a need to combine remote sensing measurements with the agricultural census, surveys, and county agricultural reports to improve the quality of agricultural statistical data in the future.

4. Conclusion

At the national scale, the interannual dynamics of cropland GPP from the satellite-based VPM model and CGP from the NBS agreed well with each other during 2000–2008, but diverged substantially during 2009–2018. The large discrepancy between cropland GPP (stagnant) and CGP (continuous increase) at the national scale during 2009–2018 has major implications for our views on grain production, food security, and agricultural policies in China and the world, which highlights the urgent need to include satellite observations to improve grain production estimates in the future. Our results show that croplands with continuous increase of GPP (~37%) were largely distributed in northern China, and GPP for 63% of croplands was stagnant, declined, or had no significant change. Further increases in cropland GPP and CGP in China would be challenging in the coming years and decades, and would be exacerbated by the geographical mismatch in the spatial distributions of croplands and water resources and the divergent temporal trends of them over time. The top grain export provinces and the largest agricultural production region (North China Plain) have strongly relied on irrigation but experienced growing water scarcity over the past decades, and they are likely to face even more challenges in water availability. Therefore, self-sufficient CGP in China is likely to remain a major concern in the coming decades. Sustainable agricultural management, for example, agro-ecological approaches (Epule and Bryant, 2015; Kerr et al., 2007; Snapp et al., 2010), and high agricultural water use efficiency are urgently needed for ensuring food security and promoting ecological sustainability.

CRediT authorship contribution statement

Fang Liu: Conceptualization, Formal analysis, Investigation, Methodology, Software, Writing – original draft. **Xiangming Xiao:** Conceptualization, Funding acquisition, Methodology, Writing – original draft. **Yuanwei Qin:** Formal analysis, Investigation, Methodology, Software, Writing – original draft. **Huimin Yan:** Funding acquisition, Writing – review & editing. **Jikun Huang:** Writing – review & editing. **Xiaocui Wu:** Methodology, Software, Writing – review & editing. **Yao Zhang:** Writing – review & editing. **Zhenhua Zou:** Writing – review & editing. **Russell B. Doughty:** Writing – review & editing.

Declaration of competing interest

The authors declare that they have no known competing financial interests or personal relationships that could have appeared to influence the work reported in this paper.

Acknowledgements

This study was supported by the Key Project of National Natural Science Foundation of China (42130505), the National Institutes of Health (1R01AI101028-02A4), and the National Science Foundation (1911955).

Appendix A. Supplementary data

Supplementary data to this article can be found online at https://doi.org/10.1016/j.scitotenv.2021.151408.

References

Aeschbach-Hertig, W., Gleeson, T., 2012. Regional strategies for the accelerating global problem of groundwater depletion. Nat. Geosci. 5 (12), 853–861.
Akaike, H., 1981. A new look at the statistical-model identification. IEEE Trans. Autom. Control 51, 22.
Bastiaanssen, W.G.M., Ali, S., 2003. A new crop yield forecasting model based on satellite measurements applied across the Indus Basin, Pakistan. Agric. Ecosyst. Environ. 94 (3), 321–340.
Brown, L.R., 1995. Who Will Feed China? Wake-up Call for a Small Planet. W.W. Norton & Company, New York and London.
Burke, M., Lobell, D.B., 2017. Satellite-based assessment of yield variation and its determinants in smallholder African systems. Proc. Natl Acad. Sci. USA 114 (9), 2189–2194.
Cassman, K.G., Dobermann, A., Walters, D.T., Yang, H., 2003. Meeting cereal demand while protecting natural resources and improving environmental quality. Annu. Rev. Environ. Resour. 28, 315–358.
Chang, Q., et al., 2019. Assessing consistency of spring phenology of snow-covered forests as estimated by vegetation indices, gross primary production, and solar-induced chlorophyll fluorescence. Agric. For. Meteorol. 275, 305–316.
Chen, H., Wang, J., Huang, J., 2014a. Policy support, social capital, and farmers' adaptation to drought in China. Glob. Environ. Chang. 24, 193–202.
Chen, X.P., et al., 2014b. Producing more grain with lower environmental costs. Nature 514 (7523), 486–489.
Cui, Y.P., et al., 2017. Temporal consistency between gross primary production and solarinduced chlorophyll fluorescence in the ten most populous megacity areas over years. Sci. Rep.-Uk 7.
Dalin, C., Hanasaki, N., Qiu, H.G., Mauzerall, D.L., Rodriguez-Iturbe, I., 2014. Water resources transfers through chinese interprovincial and foreign food trade. Proc. Natl Acad. Sci. USA 111 (27), 9774–9779.
Dalin, C., Wada, Y., Kastner, T., Puma, M.J., 2017. Groundwater depletion embedded in international food trade. Nature 543 (7647), 700-+.
Doughty, R., et al., 2021a. Global-scale consistency of spaceborne vegetation indices, chlorophyll fluorescence, and photosynthesis. J. Geophys. Res. Biogeosci. 126 (6).
Doughty, R., et al., 2021b. Small anomalies in dry-season greenness and chlorophyll fluorescence for Amazon moist tropical forests during El Nino and La Nina. Remote Sens. Environ. 253.
Du, L., et al., 2019. China's agricultural irrigation and water conservancy projects: a policy synthesis and discussion of emerging issues. Sustainability-Basel 11 (24), 7027.
Epule, E.T., Bryant, C.R., 2015. Drivers of arable production stagnation and policies to combat stagnation based on a systematic analysis of drivers and agents of arable production in Cameroon. Land Use Policy 42, 664–672.
Fukase, E., Martin, W., 2016. Who will feed China in the 21st Century? Income growth and food demand and supply in China. J. Agric. Econ. 67 (1), 3–23.
Gale, F., Service, E.R., Agriculture, U.S.D.o., 2005. China's Food and Agriculture: Issues for the 21st Century. University Press of the Pacific.
Girotto, M., De Lannoy, G.J.M., Reichle, R.H., Rodell, M., 2016. Assimilation of gridded terrestrial water storage observations from GRACE into a land surface model. Water Resour. Res. 52 (5), 4164–4183.
Gong, P., 2011. China needs no foreign help to feed itself. Nature 474 (7349), 7.
Grassini, P., Eskridge, K.M., Cassman, K.G., 2013. Distinguishing between yield advances and yield plateaus in historical crop production trends. Nat. Commun. 4.
Guo, J.H., et al., 2010. Significant acidification in major chinese croplands. Science 327 (5968), 1008–1010.
He, M., et al., 2018. Regional crop gross primary productivity and yield estimation using fused landsat-MODIS data. Remote Sens. 10 (3), 372.
Huang, J.K., Rozelle, S., 1995. Environmental-stress and grain yields in China. Am. J. Agric. Econ. 77 (4), 853–864.
Huang, J.K., Yang, G.L., 2017. Understanding recent challenges and new food policy in China. Glob. Food Sec. 12, 119–126.
Huang, J.K., Wang, X.B., Zhi, H.Y., Huang, Z.R., Rozelle, S., 2011. Subsidies and distortions in China's agriculture: evidence from producer-level data. Aust. J. Agric. Resour. Econ. 55 (1), 53–71.
Jagermeyr, J., et al., 2016. Integrated crop water management might sustainably halve the global food gap. Environ. Res. Lett. 11 (2).
Jiang, S., et al., 2017. Sustainability of water resources for agriculture considering grain production, trade and consumption in China from 2004 to 2013. J. Clean. Prod. 149, 1210–1218.
Jiao, X.Q., et al., 2016. Grain production versus resource and environmental costs: towards increasing sustainability of nutrient use in China. J. Exp. Bot. 67 (17), 4935–4949.
Jing, W.L., et al., 2019. Understanding terrestrial water storage declining trends in the Yellow River Basin. J. Geophys. Res.-Atmos. 124 (23), 12963–12984.
Joiner, J., et al., 2013. Global monitoring of terrestrial chlorophyll fluorescence from moderate-spectral-resolution near-infrared satellite measurements: methodology, simulations, and application to GOME-2. Atmos. Meas. Tech. 6 (10), 2803–2823.
Joiner, J., et al., 2014. The seasonal cycle of satellite chlorophyll fluorescence observations and its relationship to vegetation phenology and ecosystem atmosphere carbon exchange. Remote Sens. Environ. 152, 375–391.
Joiner, J., Yoshida, Y., Guanter, L., Middleton, E.M., 2016. New methods for the retrieval of chlorophyll red fluorescence from hyperspectral satellite instruments: simulations and application to GOME-2 and SCIAMACHY. Atmos. Meas. Tech. 9 (8), 3939–3967.
Kerr, R.B., Snapp, S., Chirwa, M., Shumba, L., Msachi, R., 2007. Participatory research on legume diversification with malawian smallholder farmers for improved human nutrition and soil fertility. Exp. Agric. 43 (4), 437–453.
Killick, R., Fearnhead, P., Eckley, I.A., 2012. Optimal detection of changepoints with a linear computational cost. J. Am. Stat. Assoc. 107 (500), 1590–1598.

Kuang, W., et al., 2021. Cropland redistribution to marginal lands undermines environmental sustainability. Natl. Sci. Rev., nwab091. https://doi.org/10.1093/nsr/nwab091.
Li, Q., Huang, J., Luo, R., Liu, C., 2013. China's labor transition and the future of China's rural wages and employment. Chin. World. Econ. 21 (3), 4–24.
Li, Y.X., et al., 2014. An analysis of China's grain production: looking back and looking forward. Food Energy Secur. 3 (1), 19–32.
Liu, J.Y., et al., 2005. Spatial and temporal patterns of China's cropland during 1990–2000: an analysis based on landsat TM data. Remote Sens. Environ. 98 (4), 442–456.
Liu, J.Y., et al., 2014. Spatiotemporal characteristics, patterns, and causes of land-use changes in China since the late 1980s. J. Geogr. Sci. 24 (2), 195–210.
Liu, G., et al., 2020. On the accuracy of official chinese crop production data: evidence from biophysical indexes of net primary production. Proc. Natl. Acad. Sci., p. 201919850
Lobell, D.B., Asner, G.P., Ortiz-Monasterio, J.I., Benning, T.L., 2003. Remote sensing of regional crop production in the Yaqui Valley, Mexico: estimates and uncertainties. Agric. Ecosyst. Environ. 94 (2), 205–220.
Lu, Y., et al., 2015. Addressing China's grand challenge of achieving food security while ensuring environmental sustainability. Sci. Adv. 1 (1).
Ma, J., et al., 2018. Spatial-temporal consistency between gross primary productivity and solar-induced chlorophyll fluorescence of vegetation in China during 2007–2014. Sci. Total Environ. 639, 1241–1253.
MacDonald, G.K., D'Odorico, P., Seekell, D.A., 2016. Pathways to sustainable intensification through crop water management. Environ. Res. Lett. 11 (9).
Meng, Q., et al., 2016. Growing sensitivity of maize to water scarcity under climate change. Sci. Rep.-Uk 6 (1), 19605.
Ning, J., et al., 2018. Spatiotemporal patterns and characteristics of land-use change in China during 2010–2015. J. Geogr. Sci. 28 (5), 547–562.
Pei, H.W., et al., 2015. Impacts of varying agricultural intensification on crop yield and groundwater resources: comparison of the North China plain and US High Plains. Environ. Res. Lett. 10 (4).
Ray, D.K., Ramankutty, N., Mueller, N.D., West, P.C., Foley, J.A., 2012. Recent patterns of crop yield growth and stagnation. Nat. Commun. 3.
Reeves, M.C., Zhao, M., Running, S.W., 2005. Usefulness and limits of MODIS GPP for estimating wheat yield. Int. J. Remote Sens. 26 (7), 1403–1421.
Rozelle, S., Veeck, G., Huang, J.K., 1997. The impact of environmental degradation on grain production in China, 1975–1990. Econ. Geogr. 73 (1), 44–66.
Running, S.W., et al., 2004. A continuous satellite-derived measure of global terrestrial primary production. Bioscience 54 (6), 547–560.
Scanlon, B.R., et al., 2018. Global models underestimate large decadal declining and rising water storage trends relative to GRACE satellite data. Proc. Natl Acad. Sci. USA 115 (6), E1080–E1089.
Siebert, S., et al., 2010. Groundwater use for irrigation - a global inventory. Hydrol. Earth Syst. Sci. 14 (10), 1863–1880.
Snapp, S.S., Blackie, M.J., Gilbert, R.A., Bezner-Kerr, R., Kanyama-Phiri, G.Y., 2010. Biodiversity can support a greener revolution in Africa. Proc. Natl Acad. Sci. USA 107 (48), 20840–20845.
van Ittersum, M.K., et al., 2013. Yield gap analysis with local to global relevance—a review. Field Crop Res. 143, 4–17.
Wagle, P., Zhang, Y., Jin, C., Xiao, X., 2016. Comparison of solar-induced chlorophyll fluorescence, light-use efficiency, and process-based GPP models in maize. Ecol. Appl. 26 (4), 1211–1222.
Wang, E.L., Yu, Q., Wu, D.R., Xia, J., 2008. Climate, agricultural production and hydrological balance in the North China plain. Int. J. Climatol. 28 (14), 1959–1970.
Wang, Z., Xiao, X.M., Yan, X.D., 2010. Modeling gross primary production of maize cropland and degraded grassland in northeastern China. Agric. For. Meteorol. 150 (9), 1160–1167.
Wang, H.Y., et al., 2017a. An optimal regional nitrogen application threshold for wheat in the North China plain considering yield and environmental effects. Field Crop Res. 207, 52–61.
Wang, J., Li, Y., Huang, J., Yan, T., Sun, T., 2017b. Growing water scarcity, food security and government responses in China. Glob. Food Sec. 14, 9–17.
Wei, X., et al., 2015. Is yield increase sufficient to achieve food security in China? PLoS One 10 (2).
Wiese, D.N., 2015. GRACE Monthly Global Water Mass Grids NETCDF RELEASE 5.0. Ver. 5.0. PO.DAAC, CA, USA.
Wiese, D.N., Landerer, F.W., Watkins, M.M., 2016. Quantifying and reducing leakage errors in the JPL RL05M GRACE mascon solution. Water Resour. Res. 52 (9), 7490–7502.
Wu, X., et al., 2018. Spatiotemporal consistency of four gross primary production products and solar-induced chlorophyll fluorescence in response to climate extremes across CONUS in 2012. J. Geophys. Res. Biogeosci. 123 (10), 3140–3161.
Wu, X., et al., 2021a. Spatiotemporal changes of winter wheat planted and harvested areas, photosynthesis and grain production in the contiguous United States from 2008–2018. Remote Sens. 13 (9), 1735.
Wu, X.C., et al., 2021b. Spatial-temporal dynamics of maize and soybean planted area, harvested area, gross primary production, and grain production in the Contiguous United States during 2008-2018. Agric. For. Meteorol. 297.
Xiao, X.M., et al., 2003. Uncertainties in estimates of cropland area in China: a comparison between an AVHRR-derived dataset and a landsat TM-derived dataset. Glob. Planet. Chang. 37 (3–4), 297–306.
Xiao, X.M., et al., 2004a. Satellite-based modeling of gross primary production in an evergreen needleleaf forest. Remote Sens. Environ. 89 (4), 519–534.
Xiao, X.M., et al., 2004b. Modeling gross primary production of temperate deciduous broadleaf forest using satellite images and climate data. Remote Sens. Environ. 91 (2), 256–270.
Xin, F.F., et al., 2017. Modeling gross primary production of paddy rice cropland through analyses of data from CO2 eddy flux tower sites and MODIS images. Remote Sens. Environ. 190, 42–55.
Xin, F., et al., 2019. Large increases of paddy rice area, gross primary production, and grain production in Northeast China during 2000–2017. Sci. Total Environ. 135183.
Xin, F.F., et al., 2020. Understanding the land surface phenology and gross primary production of sugarcane plantations by Eddy flux measurements, MODIS images, and data-driven models. Remote Sens. 12 (14).
Xu, X., et al., 2018. China multi-period land use and land cover remote sensing monitoring data set (CNLUCC). In:C.A.o. Data Registration and Publishing System of Resource and Environmental Science Data Center and S (Editors) http://www.resdc.cn/DOI.
Yan, H.M., et al., 2009. Modeling gross primary productivity for winter wheat-maize double cropping system using MODIS time series and CO2 eddy flux tower data. Agric. Ecosyst. Environ. 129 (4), 391–400.
Yan, M., et al., 2015. Carbon footprint of grain crop production in China - based on farm survey data. J. Clean. Prod. 104, 130–138.
Yan, H.M., et al., 2016. Potential promoted productivity and spatial patterns of medium- and low-yield cropland land in China. J. Geogr. Sci. 26 (3), 259–271.
Yan, H., et al., 2019. Tracking the spatio-temporal change of cropping intensity in China during 2000–2015. Environ. Res. Lett. 14 (3), 035008.
Yang, X.L., et al., 2015. Recharge and groundwater use in the North China plain for six irrigated crops for an eleven year period. PLoS One 10 (1).
Zhang, Y., et al., 2016. Consistency between sun-induced chlorophyll fluorescence and gross primary production of vegetation in North America. Remote Sens. Environ. 183, 154–169.
Zhang, Y., et al., 2017. A global moderate resolution dataset of gross primary production of vegetation for 2000–2016. Sci. Data 4, 170165.
Zhang, G., et al., 2020. Fingerprint of rice paddies in spatial–temporal dynamics of atmospheric methane concentration in monsoon Asia. Nat. Commun. 11 (1), 554.
Zhao, M., et al., 2020. Ecological restoration impact on total terrestrial water storage. Nat. Sustain. 4, 56–62.
Zhu, X.F., Li, Y.Z., Li, M.Y., Pan, Y.Z., Shi, P.J., 2013. Agricultural irrigation in China. J. Soil Water Conserv. 68 (6), 147a–154a.
Zou, Z.H., et al., 2018. Divergent trends of open-surface water body area in the contiguous United States from 1984 to 2016. Proc. Natl Acad. Sci. USA 115 (15), 3810–3815.